Techniques to Improve the CLEAN Deconvolution Algorithm

by AVRAHAM FREEDMAN, RANJAN BOSE *and* BERNARD D. STEINBERG

Valley Forge Research Center, Moore School of Electrical Engineering, University of Pennsylvania, Philadelphia, PA 19104, U.S.A.

ABSTRACT: *The CLEAN algorithm was introduced in radio astronomy as a means to overcome the shadowing of small targets by the sidelobes of the point spread function (PSF) of a strong target. The idea was further used in microwave imaging where the concept of coherent CLEAN was introduced. The classical CLEAN algorithm is limited to a case where the targets are isolated. Techniques to overcome this limitation are presented in this paper. These techniques include PSF correlation to improve the estimation of target locations and intensities, sequence CLEAN (S-CLEAN) which improves the detection of true targets and suppresses the detection of false ones, and iterative CLEAN (ICLEAN) which uses knowledge about a target to improve the estimation of other targets' parameters. Emulation, using real experimental data, shows that a significant improvement can be achieved using these techniques.*

I. Introduction

Definitions

The problem to be solved is the deconvolution problem. We are using radar imaging terminology, though the solution is applicable to a large variety of problems.

Let a *scene* $s(t)$ to be composed of N point targets, in which the nth target reflects with a complex amplitude $\mathbf{A}_n$. Then

$$s(t) = \sum_{n=1}^{N} \mathbf{A}_n \delta(t-t_n), \tag{1}$$

where $\delta(t)$ is the Dirac delta function. The scene is imagined by an imaging system defined by its point spread function (PSF) $p(t)$, which we assume to be known, but arbitrary. The input scene is convolved by that PSF and yields the *image* $I(t)$:

$$I(t) = \sum_{n=1}^{N} \mathbf{A}_n p(t-t_n) + n(t) \tag{2}$$

with $n(t)$ complex, Gaussian white noise, with zero mean and spectral power density N_0.

0016-0032(95)00079-8

The goal of CLEAN, which is a deconvolution algorithm, is to reconstruct the original scene $s(t)$.

Background and motivation

Deconvolution techniques have been used in seismic exploration and in radio astronomy for several decades. Our original problem involves a PSF with some of the spectral components missing. Because of this we could not use a classical technique such as inverse filtering (**1**). Another classical technique is homomorphic filters (**2**), which converts the convolved signals into an additive sum of the components. This technique requires that the scene and the PSF have a substantially different spectrum, which is not the case in our problem.

The CLEAN deconvolution algorithm, to be described in the next section, was first introduced in radio astronomy as a way to overcome the shadowing of small targets by the sidelobes of the PSF of a strong target (**3**). The idea was further used in microwave imaging in (**4**, **5**), which introduced the concept of coherent CLEAN.

The problem can also be expressed as a parameter estimation problem. In this case a minimum mean square error estimator is computed by searching for the set of parameters $\{\hat{\mathbf{A}}_n, \hat{t}_n\}|_{n=1}^{N}$ which minimizes the error:

$$\int_{-\infty}^{\infty} \left| I(t) - \sum_{n=1}^{N} \hat{\mathbf{A}}_n p(t-\hat{t}_n) \right|^2 \mathrm{d}t. \tag{3}$$

In our case, where the noise is assumed to be Gaussian, this is also the maximum likelihood estimator.

A solution to this type of problem is given in (**6**), where the number of targets is known, and where the second derivative of $p(t)$ exists and is known as well. Minimizing (3) results in a set of nonlinear equations which are solved numerically. Reference (**6**) has a special interest for us as it uses CLEAN to provide initial estimates for the target parameters. Another solution is given in (**7**) where a quantized discrete representation is given, and the number of targets is assumed to be equal to the number of pixels in the image. In this case the problem is reduced to a simple linear problem and it can be directly solved.

In this representation, the problem is very similar to the problem of spectral estimation (**8**). The main difference is that spectral estimation was designed to achieve good estimates of target parameters even within the basic resolution cell (a super resolution problem), while the CLEAN algorithm was originally designed to overcome the problem of high sidelobes and improve the image dynamic range. However, CLEAN can be used for super resolution (**7**), and spectral estimation techniques can be used to improve the image dynamic range. Following (**7**), the steps of the CLEAN algorithm can be viewed as representing an indirect approach of the solution of the same minimum mean square error problem. CLEAN was apparently formulated with the attitude that for real images the number of simultaneous equations that would have to be solved for the error to be minimized is prohibitively large.

The CLEAN algorithm

The coherent CLEAN algorithm is described as follows:

(1) Find the brightest point in the image (the m^{th} point).
(2) Estimate its complex amplitude $\hat{\mathbf{A}}_m$ and location $\hat{t}_m$.
(3) Form a new image by subtracting the complex PSF weighted by the complex amplitude (or a fraction γ thereof) from the location of the brightest point:

$$I_m(t) = I(t) - \gamma \hat{\mathbf{A}}_m p(t - \hat{t}_m). \tag{4}$$

The new image is devoid of the strongest target as well as its high sidelobes, thus exposing weaker targets that were previously submerged in the sidelobes. The coefficient γ, called the loop gain, is the fraction of the source amplitude subtracted in each iteration. The loop gain is chosen smaller than unity for stability of the CLEAN procedure.
(4) Repeat the procedure on the next brightest target, and so on.
(5) Stop this procedure when all targets are canceled or noise level is reached.
(6) Develop a list of locations and the respective complex amplitudes of the targets canceled.
(7) Form the CLEAN image by convolving the mainbeam of the point spread function with properly sized δ-functions located at the target locations.

The above algorithm is based on the following assumptions:

(1) the targets are independent and isolated;
(2) the brightest point in the image is the response to a real target and not an accidental constructive interference of the sidelobe responses;
(3) the sidelobe and noise interference are negligible compared to a mainbeam signal; thus sidelobes and noise do not affect target parameter estimation.

These assumptions do not hold very well in the case of high resolution imaging of real-life targets as most radar targets are contiguous. It is likely that the brightest point (highest peak) is an artifact rather than a response to a real target, and even if a real target is detected the peak of its response shifts considerably due to interference and noise. Canceling a spurious peak can cause an addition of other spurious peaks, thus making Coherent CLEAN unstable. Figure 1 demonstrates these problems. The scene, depicted in Fig.1(a), contains three targets which are convolved with a PSF of which the magnitude is presented in Fig. 1(b). The resulting image with noise in Fig. 1(c) shows an abundance of spurious peaks and wrong locations (the original targets are denoted by asterisks). The scene reconstructed by the CLEAN algorithm, presented in Fig. 1(d), hardly resembles the original one.

Three techniques are considered in this paper to improve the performance of the CLEAN algorithm:

(1) PSF correlation, which improves the estimation of target location and complex amplitude;
(2) S-CLEAN, which reduces the chance of choosing an artifact as a real target;

Vol. 332B, No. 5, pp. 535–553, 1995

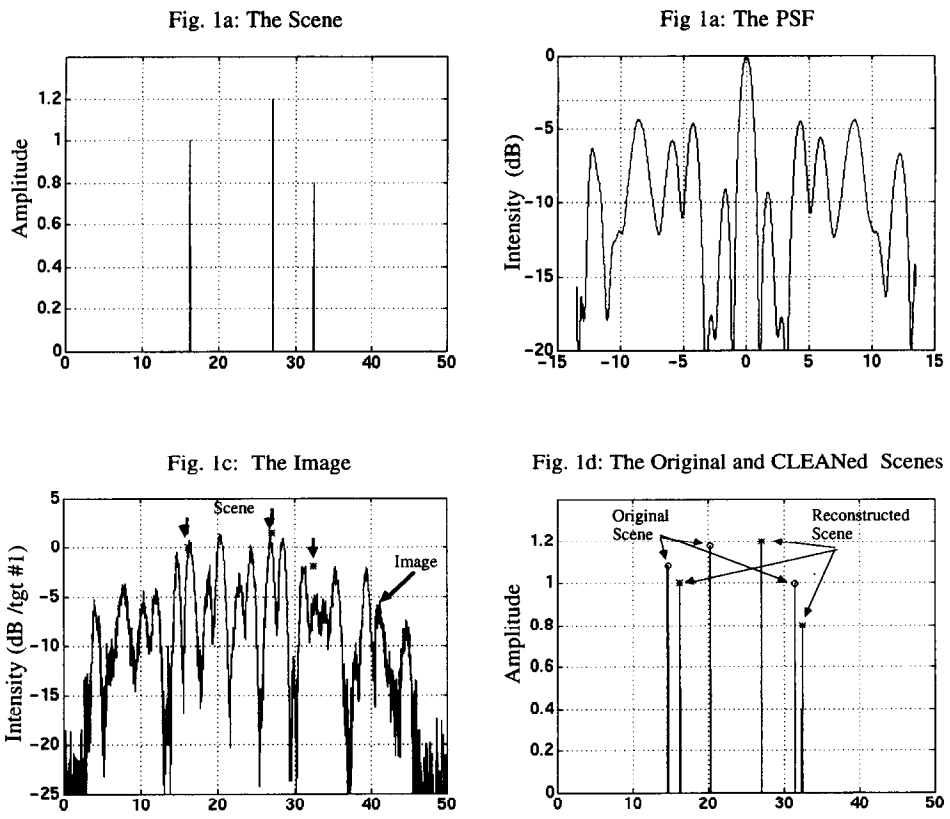

FIG. 1. An example to demonstrate the terms *scene* and *image* and the problems encountered by the CLEAN deconvolution algorithm.

(3) ICLEAN, which further improves target parameter estimation, after detection of other targets.

These techniques are introduced and analysed in the following sections.

The minimal target mass criterion

Before we proceed with the description of the algorithms, it is necessary to define a criterion to evaluate the quality of image reconstruction. Consider the total energy of the residual image I_m:

$$M_m = \int_{-\infty}^{\infty} |I_m(t)|^2 \, dt, \tag{5}$$

which we call the target mass. For an image containing a number of strong targets, it is the energy associated with the targets that contributes the most to the target mass. Thus the smaller the mass in the image the better the subtraction. Therefore it is intuitively appealing to use it as a "figure of demerit" for a residual image. As shown later, the target mass is highly correlated with the error in target location

estimation. As target location is a key parameter in our application, we found target mass most useful.

II. The PSF Correlation Algorithm

Derivation

Using the target mass criterion, finding the values of the target location and target amplitude which minimize the residual target mass is straightforward. The residual mass can be written as

$$\begin{aligned} M_m &= \int_{-\infty}^{\infty} \{I(t)-\hat{\mathbf{A}}_m p(t-\hat{t}_m)\}\{I(t)-\hat{\mathbf{A}}_m p(t-\hat{t}_m)\}^* \,\mathrm{d}t \\ &= M+|\hat{\mathbf{A}}_m|^2 M_p - 2\,\mathrm{Re}[\hat{\mathbf{A}}_m R^*_{pI}(\hat{t}_m)] \\ &= M+|\hat{\mathbf{A}}_m|^2 M_p - 2|\hat{\mathbf{A}}_m|\,|R_{pI}(\hat{t}_m)|\cos[\hat{\alpha}_m-\phi(\hat{t}_m)], \end{aligned} \tag{6}$$

where M is the original image mass, M_p is the mass of the point spread function and $R_{pI}(\hat{t}_m)=\int_{-\infty}^{\infty} p^*(t-\hat{t}_m)I(t)\,\mathrm{d}t$ is the cross-correlation function between the image and the PSF. We also denoted the phase of $\hat{\mathbf{A}}_m$ and $R_{pI}(\hat{t}_m)$ by α_m and $\varphi(\hat{t}_m)$, respectively. Observing (6), it can be seen that the minimal value of the residual mass is reached when:

(1) the location estimation is given by the value of $\hat{t}_m$ which brings the absolute value of cross-correlation $R_{pI}(\hat{t}_m)$ to a maximum;
(2) the phase of the complex amplitude estimation is taken as equal to the phase of the cross-correlation function, namely $\hat{\alpha}_m=\varphi(\hat{t}_m)$;
(3) the absolute value of the complex amplitude is taken as $|\hat{\mathbf{A}}_m|=|R_{pI}(\hat{t}_m)|/M_p$.

The last two points can simply be written as

$$\hat{\mathbf{A}}_m=\frac{R_{pI}(\hat{t}_m)}{M_p},$$

namely the complex amplitude estimation is taken as the value of the cross-correlation function estimated at its peak, and normalized by the PSF energy.

This result implies that the estimation procedure used is conventional CLEAN, which estimates the location and complex amplitude as their value of the image peaks, does not minimize the residual target mass. It is evident that the closer the PSF is to an impulse function the closer are the results obtained using the two methods.

For algorithm stability purpose, it is customary to subtract only a fraction, $0<\gamma\leqslant 1$, from the original image. The residual mass, resulting from substituting

$$\hat{\mathbf{A}}_m=\gamma\frac{R_{pI}(\hat{t}_m)}{M_p}$$

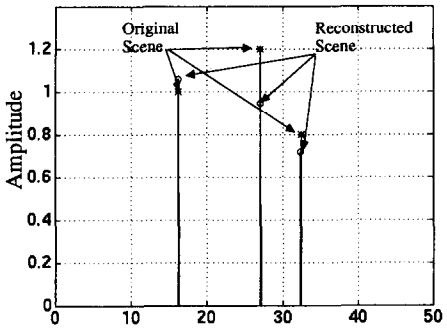

FIG. 2. Original scene and a scene reconstructed by PSF correlation.

in this case is

$$M_m = M-(2-\gamma)\gamma\frac{|R_{pI}(\hat{t}_m)|^2}{M_p} \tag{7}$$

which reaches a minimum when $\gamma = 1$.

The PSF correlation algorithm is actually a matched filter. As such, it is theoretically known to perform optimally in a white Gaussian noise environment. When the CLEAN algorithm is applied to a very dense target environment, the sidelobe interference of many target responses can be modeled as white noise, and thus PSF correlation is optimal as well, provided the assumption is accurate. In a less dense environment PSF correlation is no longer optimal. However, it is always the algorithm which will yield the maximal reduction in target mass, and in that sense it is optimal. Note that no assumption was made on the PSF being used; hence, even if the PSF is not exactly known, the PSF correlation will produce the residual image with the minimal target mass (though target parameters may be erroneously estimated).

The advantage of using PSF correlation is demonstrated in Fig. 2, where the same scene as in Fig. 1 is reconstructed with a CLEAN algorithm, using PSF correlation for target parameter estimation. Comparing it to Fig. 1(d) shows a much better reconstruction of the original scene: the target locations are estimated quite accurately, although the amplitude estimation was not as accurate.

Residual mass and location error correlation

The correlation between the residual mass and the target location error is an important subject. In order to distinguish between the contribution of noise to the contribution of other targets, we shall write (1) as follows

$$I(t) = \mathbf{A}_m p(t-t_m) + \sum_{\substack{n=1 \\ n\neq m}}^{N} \mathbf{A}_n p(t-t_n) + n(t) = \mathbf{A}_m p(t-t_m) + I_{\hat{m}} + n(t). \tag{8}$$

$I_{\hat{m}}$ is defined as the complementary image to the image of the mth target. The second term in (7) can be evaluated as

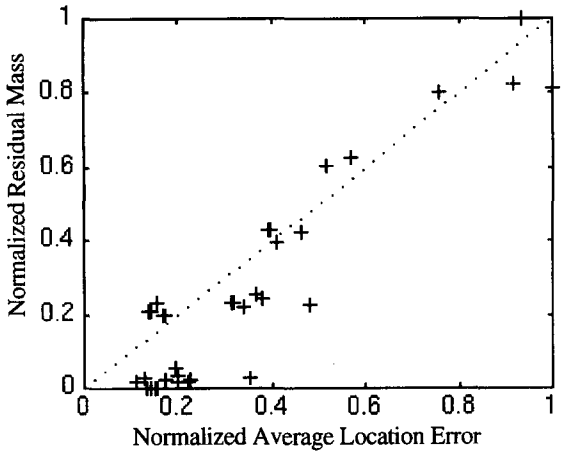

FIG. 3. The normalized residual mass and the normalized average location error vs 100 different paths.

$$R_{pI}(\hat{t}_m) = \int_{-\infty}^{\infty} p^*(t-\hat{t}_m)[\mathbf{A}_m p(t-t_m) + I_{\hat{m}}(t) + n(t)]\,dt$$

$$= \mathbf{A}_m R_p(\Delta) + R_{pI_{\hat{m}}}(\hat{t}_m) + R_{pn}(\hat{t}_m), \tag{9}$$

where $\Delta = \hat{t}_m - t_m$ signifies the error in the estimation of the true target location. If, in addition, the mth target is assumed to be a strong one and the contributions of adjacent targets in its vicinity are small, the main contribution to the correlation function in (9) results from the first term, which is a function of the error in the target location estimation, Δ. As an auto-correlation function, its amplitude peaks at $\Delta = 0$. It is clear that for the assumptions stated above, the target mass criterion is highly correlated with error in target location estimation, which is the primary parameter in most practical cases.

The following simulation demonstrates the correlation. In this simulation an image composed of six targets, each of approximately 20 dB SNR, was synthesized using a point spread function of -10 dBc average sidelobe level. The targets are located randomly and a single realization of noise is used in the example. The CLEAN algorithm was used to extract those targets. The subtraction was performed in 100 different orders (paths). The simulation result is given in Fig. 3, in which we have plotted the normalized residual mass vs the normalized average location-error. We observe that the paths with small residual masses are also the paths that result in small average location errors. These simulation results justify our use of target mass criterion as a measure of location errors, and hence the measure of performance.

Comparison of PSF correlation and peak location estimation

The following simulation compares the location error achieved using PSF correlation with that of the standard peak location, for a variety of signal-to-noise levels and the PSF sidelobe level

In this simulation an image consisting of six point targets convolved with a PSF with variable average sidelobe level and corrupted with noise is used as an input to the target parameters estimation step of the CLEAN algorithm. Target 1 is located far from the rest; thus it is affected mainly by noise. Target 2 is located far enough from target 3 such that the sidelobe interference caused by target 3 in the vicinity of the peak of target 2 is negligible. The rest of the targets are located close together. Thus the estimation of their locations is highly affected by the average sidelobe level.

The following figures present the r.m.s. location errors, normalized to the main lobe width of the PSF, as a function of the SNR (taken as the ratio of the first target energy to the noise variance) and the average sidelobe level (ASL). The r.m.s. averaging was performed over 100 Monte Carlo runs of the simulation. In each run, the PSF and the noise realization were chosen randomly. The location estimation error associated with the conventional peak estimation method is presented as a white mesh surface, while the error resulting from an estimation based upon the peak of the correlation is presented by a black surface. The diagrams at the top of each figure show schematically the case presented.

Figure 4(a) below shows the location error of target 1. Being isolated, the target

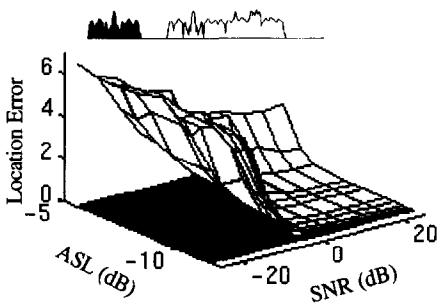

Fig. 4a: An Isolated target

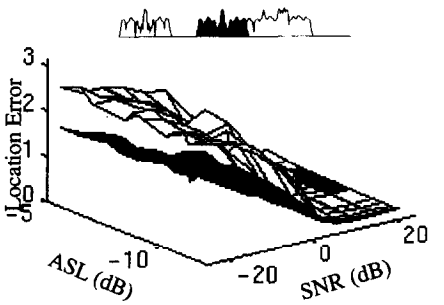

Fig. 4b: A marginally effected target

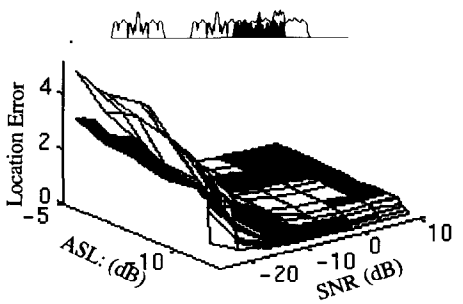

Fig. 4c: Low density environment

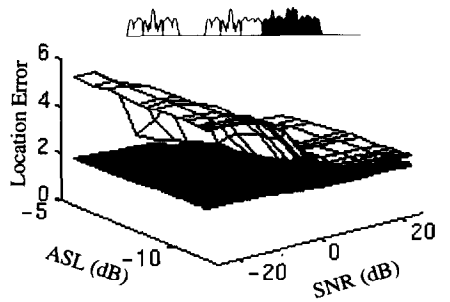

Fig. 4d: High Density Environment

FIG. 4. Comparison of target location error as a function of SNR and average sidelobe level between conventional peak estimation (white mesh) and PSF correlation estimation (black surface).

is not affected by other targets' PSFs. A low error is achieved for the high SNR–low ASL case. When the ASL rises and the SNR drops, the peak algorithm may mistake a sidelobe as the peak, resulting in a large location error. The location error achieved using the correlation procedure is much lower, as expected from estimation theory.

Figure 4(b) presents the r.m.s. error in location estimation of target 2. This target is only marginally affected by sidelobe interference. For high SNR, the conventional estimation using the peak of the image intensity is better than the one based upon the correlation in high SNR. However, when the SNR drops, the PSF correlation method is superior.

Figure 4(c) presents the location error of target 3. This target is affected by sidelobe interference resulting from a small number of targets. In this case also the correlation proves to be superior to the conventional estimation using the peak of the image intensity for the low SNR case but the results are comparable for high SNR values.

Figure 4(d) presents the average r.m.s. error in the estimation of the location targets 3–6. In this case the effect of the sidelobe interference can be modeled as noise. The PSF correlation performed better than the peak estimation over all the range of the SNR and ASL.

III. Sequence CLEAN

The S-CLEAN algorithm

S-CLEAN is a tree search algorithm which chooses the best possible sequence of target cancellations so as to maximize target mass cancellation (**9, 10**). It works on the following assumption. Even if the brightest target (highest peak) is an artifact, it may be possible that a smaller peak corresponds to a response to a real target. It is logical to cancel this smaller peak first. Canceling a real target causes energy to be subtracted from the main lobe as well as from the sidelobes. This will cause sidelobe artifacts to reduce, which may further expose more peaks corresponding to real targets.

The objective of the algorithm is to estimate true target locations and subtract out the main lobe as well as the sidelobes of the PSF from that location. Removal of sidelobes exposes weaker peaks for subtraction in subsequent stages. It will be shown later that if we can subtract out the PSF from the correct location, maximum target mass cancellation occurs.

The following example illustrates the working of S-CLEAN. Suppose there are two closely spaced point sources, A and B. Due to the coherent interaction of their sidelobes a third peak C is formed that is higher than both A and B. There are six possible sequences with which to cancel the three peaks (ABC, ACB, BCA, BAC, CAB, CBA). Of these, the sequence CLEAN algorithm finds that particular sequence which results in maximum target mass cancellation. This example is over-simplified and assumes that the coherent interactions do not change the peak locations substantially. Sequence CLEAN works step by step and maintains a record of the target mass canceled at each step.

Vol. 332B, No. 5, pp. 535–553, 1995

Algorithm for sequence CLEAN

The sequence CLEAN algorithm is given here, without loss of generality, in one dimension only. It can be summarized as follows:

(1) At the kth step of the algorithm, chose m highest peaks in the image for all the M_k surviving images ($M_k \leqslant m^k$).
(2) For the ith peak ($i=1,\ldots,m$) in the jth image ($j=1,\ldots,M_k$), subtract a fraction γ of the PSF $p(x)$ from the image $s_{k,j}(x)$ to form the new image $s^i_{k+1,j}(x) = s_{k,j}(x) - \gamma p(x-x_i)$.
(3) Compute the target mass $T^i_{k+1,j}$ remaining in the partially cleaned image $s^i_{k+1,j}(x)$, where $T^i_{k+1,j} = \int_{-\infty}^{\infty} s^i_{k+1,j}(x) s^i_{k+1,j}{}^*(x)\,dx$. A "surviving image" will be declared only if $T^i_{k+1,j} \leqslant T_{k,j}$, where $T_{k,j} = \int_{-\infty}^{\infty} s_{k,j}(x) s_{k,j}{}^*(x)\,dx$.
(4) Repeat steps (1)–(3) until there are no surviving images.
(5) Choose that sequence of target cancellation which results in the minimum residue $T^i_{K,j}$ where K is the depth of the tree for which the minimal residue is achieved.
(6) For this sequence, develop a list of the locations and respective amplitudes of the targets canceled.
(7) Form the clean image by convolving the mainbeam of the PSF with properly sized spikes at target locations.

Complexity of sequence CLEAN

As mentioned earlier, sequence CLEAN is a tree search algorithm. Its complexity grows exponentially with the number of peaks chosen at each step of the algorithm. Larger m results in better performance but is expensive in terms of time and complexity. The number m is heuristically determined.

Among the large number of paths in the tree search diagram, only a very small number of paths lead close to the solution. Most of the search paths result in addition of target mass after a few steps and are declared unstable. Such paths are terminated as soon as the point of instability is reached. Consequently, the daughter paths that would have been generated also get eliminated. Figure 5 illustrates this point. The continuous lines represent stable paths; the broken lines show the paths where addition of mass takes place. These paths and their daughter paths are eliminated. This reduces the computation time considerably as only a small number of search paths are followed to the bottom of the m-ary tree. It can be seen from Fig. 5 that one of the paths in the m-ary tree is the coherent CLEAN. Coherent CLEAN corresponds to the case $m = 1$, and is depicted by the bold lines in the figure. Coherent CLEAN is thus a subset of sequence CLEAN.

Simulation results

The simulated scene of Fig. 6(a) consists of five targets, of which four are closely spaced in range. The targets are of unequal heights (1.0, 1.0, 1.1, 0.9, 1.0). Pulse compression has been used to synthesize a bandwidth of 200 MHz, giving a range resolution of 0.75 m. The first target is isolated from the cluster of the other four targets. The spacing between the four closely located targets is 1.05 m. For a bandwidth of 200 MHz these three targets are just resolvable. Thus, these point sources closely simulate a contiguous target.

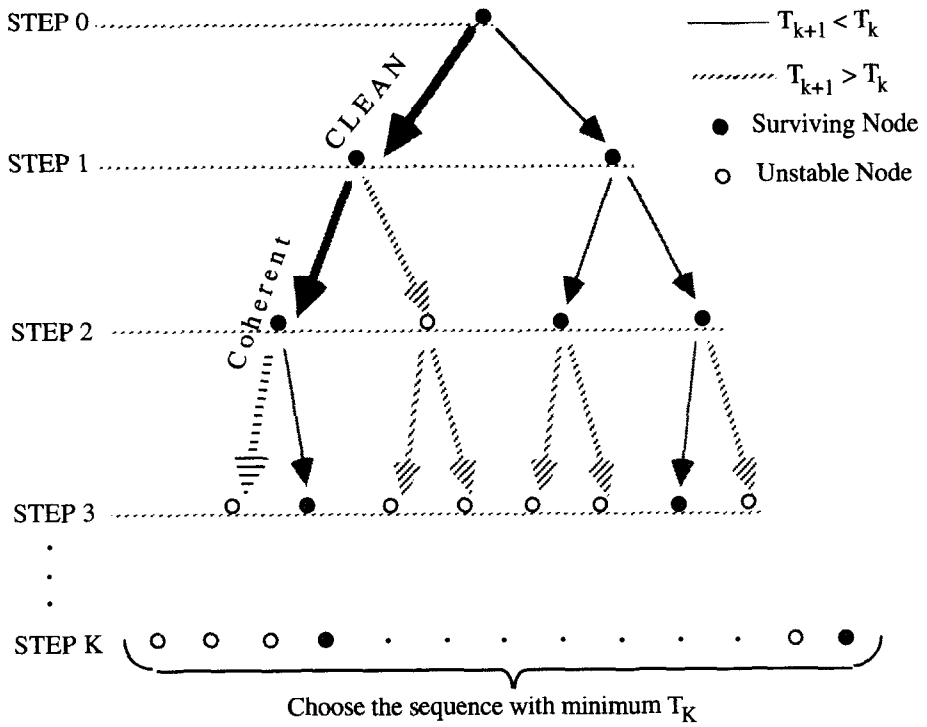

FIG. 5. Example of sequence CLEAN for $m = 2$, where m is the number of highest image peaks selected at each iteration. Note that coherent CLEAN is one of the sequences in sequence CLEAN.

$N = 10$ randomly selected subbands were used to image these targets. The reconstructed 1-D image (range profile) is given in Fig. 6(b). The PSF used in the experiment was obtained from the image of the isolated target and it can be seen that the waveform used results in very high range sidelobes. This is due to the 50% spectral thinning, as presented in (**11**). A -15 dB additive noise (relative to target 1) has been added to the raw data to simulate realistic conditions.

The coherent CLEAN algorithm was then applied to the unCLEAN image (Fig. 6b) with loop gain $\gamma(1)$ of 0.3, the algorithm failed to converge in this case. Figure 6(c) shows one of the intermediate stages. It can be seen that coherent CLEAN was not able to recover the target locations and the respective heights correctly. The coherent CLEAN algorithm also called several spurious target peaks.

The result of applying sequence CLEAN to the same image (Fig. 6b), with the same noise realization, is given in Fig. 6(d). In this case $m = 4$ and the loop gain $\gamma = 0.8$, which is more efficient than the value $\gamma = 0.3$ used for the coherent CLEAN example. Sequence CLEAN detected the targets and located them correctly. The target heights have been determined with average error of 16%

Figure 7 shows the variation of the residual target mass as a function of step number. The ordinate represents the normalized target mass in the image. Here we have shown five typical paths from the m-ary tree search. Three paths are stable,

Vol. 332B, No. 5, pp. 535–553, 1995

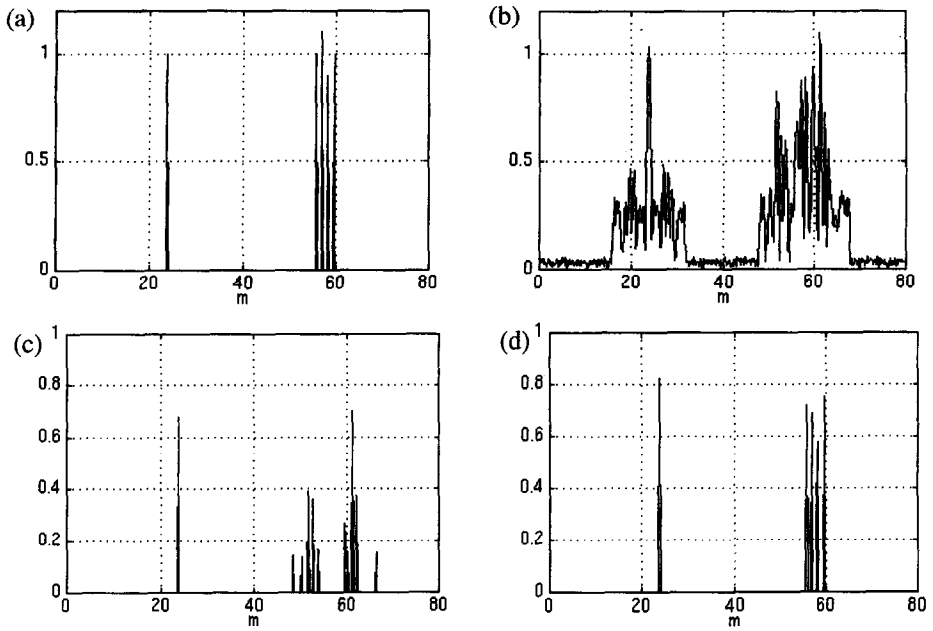

FIG. 6. (a) Location of targets in the simulated scene. (b) Reconstructed image (range profile) corresponding to target scene shown in (a). (c) Target locations and heights as recovered by coherent CLEAN. (d) Target locations and heights as recovered by sequence CLEAN.

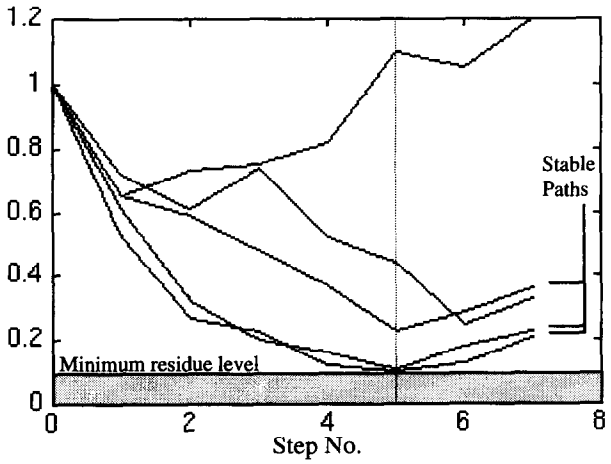

FIG. 7. Typical plots of the residual target mass in the image at different stages of the algorithm. The dotted lines correspond to the unstable paths. The minimum residue level depends on the noise originally present in the image and the noise in the PSF.

one of which leads to the minimum residual mass. The other two paths result in addition of target mass before all the five targets in the scene have been detected. It can be seen that after all five targets have been canceled out, the target mass in

the stable paths increases. This is caused by subtracting out an artifact as all the true targets have already been canceled out. In these simulations we have used a large value of the loop gain ($\gamma = 0.8$) which causes almost all of the target to be subtracted out in a single step. The minimum residue level depends on the original scene itself, the noise in the original scene and the uncertainty in the knowledge of the PSF.

IV. The ICLEAN Algorithm

The algorithm

The iterative CLEAN (ICLEAN) deconvolution procedure is introduced in (**12**). Its purpose is to avoid the errors in the estimation of target locations and intensities due to interference from adjacent targets. The procedure is based upon the fact that removing a PSF associated with a target will reduce the interference that caused an error in the location and complex amplitude estimation of other targets. Thus if we add the PSF of a previously detected target back to the CLEANed image we should be able to achieve a better estimate of the target location and amplitude.

The image resulting from the subtraction of M targets is

$$I_M(t) = \sum_{i=1}^{M} \varepsilon_i(t) + \sum_{i=M+1}^{N} \mathbf{A}_i p(t-t_i) + n(t), \tag{10}$$

where $\varepsilon_i(t) = \mathbf{A}_i p(t-t_i) - \hat{\mathbf{A}}_i p(t-\hat{t}_i)$ is the residue associated with the wrong estimation of the ith target location and amplitude. We assume the cancellation was good enough, so that according to some norm, $|\varepsilon_i(t)| \ll |\mathbf{A}_i p(t-t_i)|$.

As one of the M targets (the jth target, $j \leqslant M$) is added back to the CLEANed image, I_m, its contribution is restored:

$$I_{Mj} = I_M + \hat{\mathbf{A}}_j(t-\hat{t}_j) = \mathbf{A}_j p(t-t_j) + \sum_{\substack{i=1 \\ i\neq j}}^{M} \varepsilon_i(t) + \sum_{i=M+1}^{N} \mathbf{A}_i p(t-t_i) + n(t). \tag{11}$$

The interference in the region of t_j is given by the last three terms in (11). The complex amplitude and the location for the jth target were originally estimated when the interference in its region was

$$\sum_{i=1}^{j-1} \varepsilon_i(t) + \sum_{i=j+1}^{M} \mathbf{A}_i p(t-t_i) + \sum_{i=M+1}^{N} \mathbf{A}_i p(t-t_i) + n(t). \tag{12}$$

We see that the residue $\varepsilon_i(t)$ replaces the original response $\mathbf{A}_i p(t-t_i)$ in (11) for all the targets between $j+1$ and M. As we assumed the residue to be smaller than the original response, we can conclude that the jth target parameters can now be better estimated.

The ICLEAN algorithm calls for an addition of another step in the CLEAN algorithm following step 3, in which, for each previously detected target (in random

Vol. 332B, No. 5, pp. 535–553, 1995

order):

(1) the PSF located at the estimated position and weighted by the previously estimated complex amplitude is added to the residual image to form the image I_{M_j};
(2) the target location and amplitude are estimated again;
(3) the PSF, located in the new estimated location and weighted by the new complex amplitude, is subtracted from the image I_{M_j} to form a new residual image.

Simulation description

In (**12**) a comparison (by simulation) is presented between ICLEAN and the conventional CLEAN. The comparison was made on an image of a complex target (F-16 plane), convolved with a high sidelobe PSF. In this paper we study the effects of the main parameters of a scene on the efficiency of the ICLEAN algorithm. This study is made by simulating a simple scene containing only two point targets, convolved with a well-known sinc function as a PSF.

The image to be CLEANed is composed of two targets. Target 1 is of amplitude 1 and 0 phase and located at the origin while the other (target 2) is of a variable amplitude $A_2 e^{j\phi}$ and located at $t = \Delta t$.

$$I(t) = \frac{\sin(\pi t)}{\pi t} + A_2 e^{j\phi} \frac{\sin[\pi(t-\Delta t)]}{\pi(t-\Delta t)} + n(t), \tag{13}$$

where $n(t)$ is a white Gaussian noise. The simulation applies a gain one CLEAN and ICLEAN and compares them, using the residual mass criterion, described above, which is correlated to the error in target location.

Figures 8 and 9 demonstrate the advantage of ICLEAN over conventional CLEAN, in a noiseless scenario. Figure 8 shows the residual mass (normalized to the original image energy), as a function of the amplitude ratio and the distance between the two targets. It is clear that both algorithms perform very well when either the amplitude ratio or the distance between the targets is large. Using ICLEAN, it is possible to eliminate the effects of the first sidelobe interference, and even reduce the effect of main lobe interference.

Figure 9 shows the normalized residual mass as a function of the amplitude ratio and the phase difference ϕ, for a distance of $\Delta t = 1$. It can be observed that on certain phases (around 90°) the CLEAN algorithm performs quite well. However, this conclusion must be taken very cautiously as this simulation used a real PSF, which added no phase error to the estimation.

Figure 10 compares conventional CLEAN and ICLEAN for three levels of SNR (which is the ratio of target 1 energy to the noise variance) and for two different target distances. In all the cases $A_2 = 1$ and $\phi = 0$. It shows the probability distributions (histograms) of the residual target mass, which were obtained from 8000 Monte Carlo simulations performed for each of the six cases. The distribution for the ICLEAN residual mass is shown in a solid line, while that of the CLEAN is shown in a dashed line. The overall shape of the distributions are Ricean in nature. For a high (30-dB) SNR, shown in Fig. 10(a,b) for distances $\Delta t = 2$ and $\Delta t = 1$

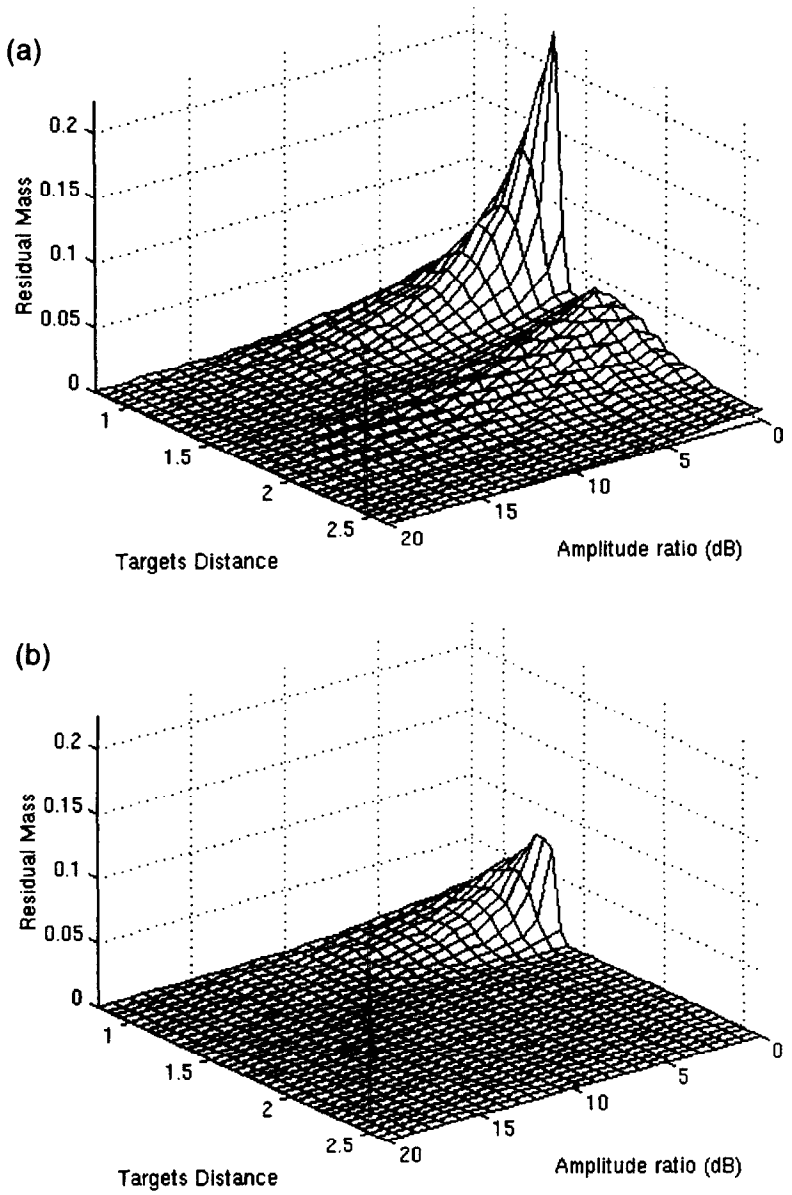

FIG. 8. Comparison of CLEAN and ICLEAN, noiseless scenario, $\phi = 0$.

respectively, the ICLEAN distribution is skewed towards a lower value and thus is superior to the CLEAN. For a 20-dB SNR (Fig. 9c,d), the ICLEAN is better than CLEAN for the $\Delta t = 2$ case, where the first sidelobe is the main cause of interference, but comparable to CLEAN when the distance is only 1. For a 10-dB SNR, the noise is the main cause of interference, and it obscures the first sidelobe. The basic premise of ICLEAN is that the sidelobes are the main cause of inter-

Vol. 332B, No. 5, pp. 535–553, 1995

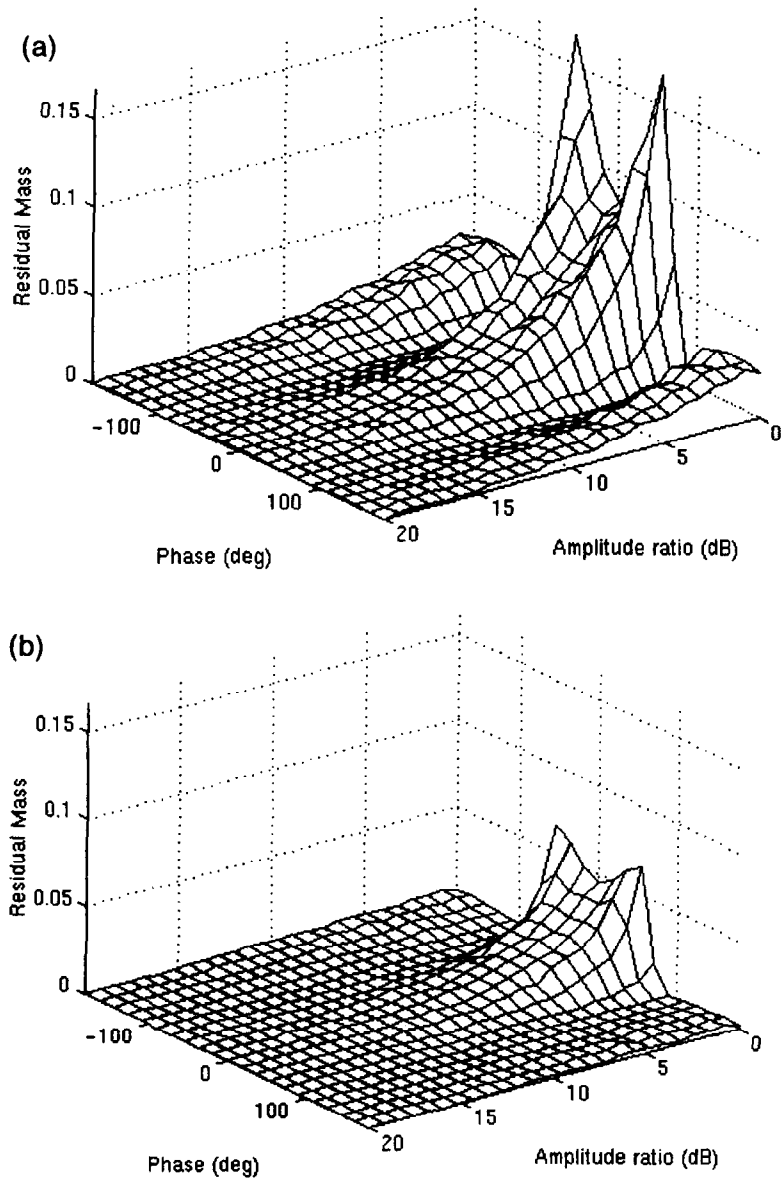

FIG. 9. Comparison of CLEAN and ICLEAN, noiseless scenario, $A_2 = 1$, $\Delta t = 1$.

ference. This premise fails in this case. Hence the performance of ICLEAN is even worse than that of CLEAN.

V. Simulation Including all Techniques

To see the contribution to the CLEAN algorithm of the three techniques discussed, we performed the following simulation. Starting with the scene described

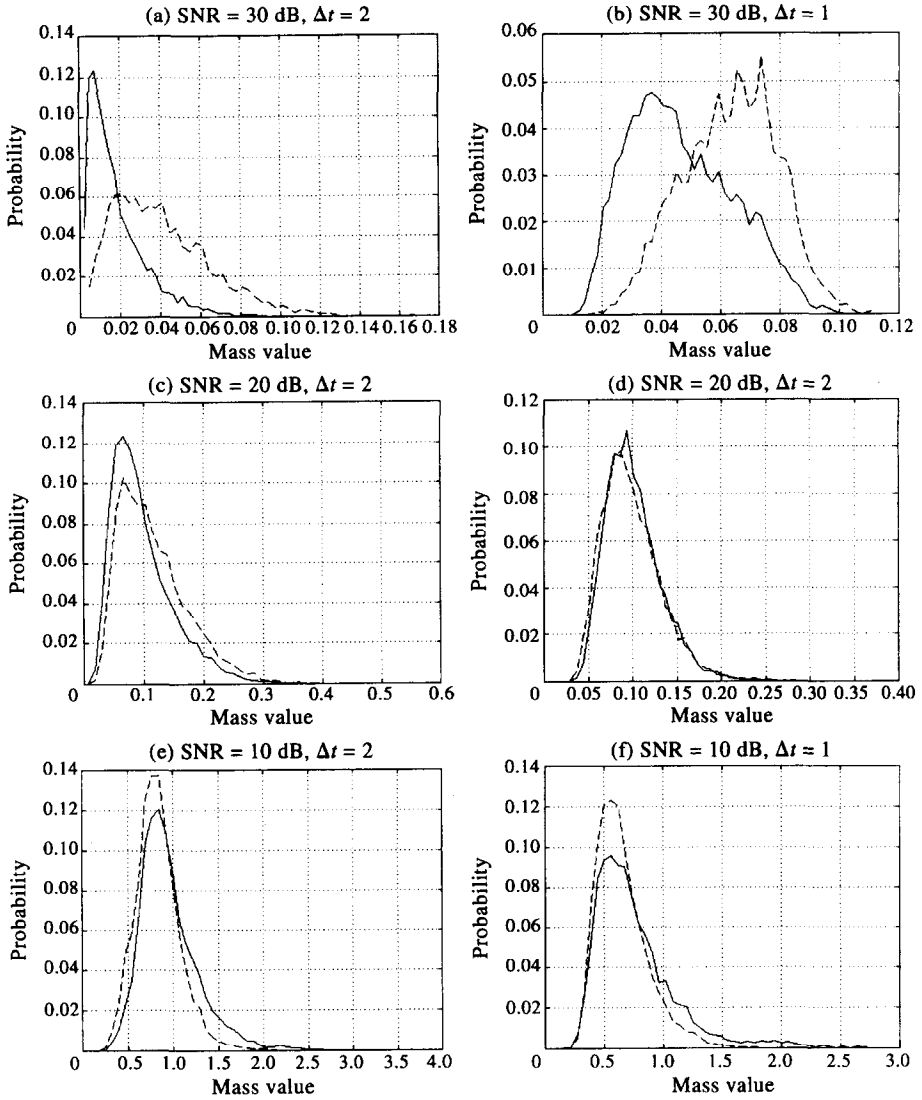

FIG. 10. Residual mass probability distribution of CLEAN (dashed line) and ICLEAN (solid line) as a function of SNR and distance.

in Fig. 6(a), we produced four different images with varying sidelobe level and SNR: high SNR (30 dB) and low ASL (−20 dBc), high SNR (30 dB) and high ASL (−8 dBc), low SNR (10 dB) and low ASL (−20 dBc) and low SNR (10 dB) and high ASL (−8 dBc). To these images we applied: CLEAN alone; sequence CLEAN; S-CLEAN, using PSF correlation to locate the targets; and S-CLEAN with PSF correlation and ICLEAN at the final stage to improve the results. The ratio of the energy in the residual image to the original image energy (over the ratio of the noise alone) is given in Table I as an indicator of the performance of

TABLE I
A comparison of various algorithms applied upon different images

	High SNR, low ASL	High SNR, high ASL	Low SNR, low ASL	Low SNR, high ASL
CLEAN	0.03	0.15	0.05	0.26
S-CLEAN	0.03	0.12	0.02	0.18
S-CLEAN PSFC	0.02	0.1	0.001	0.1
S-CLEAN PSFC, ICLEAN	0.005	0.02	0.001	0.1

the various algorithms. The numbers given are for a single case (single PSF and noise realizations) and may vary greatly in other cases.

The first image, where the interference is low, presents no problem to the CLEAN algorithm. All target locations were estimated correctly, thus the S-CLEAN did not provide any improvement. Still the amplitudes were wrongly estimated. PSFC and ICLEAN improved the complex amplitude estimation and thus provided a better target cancellation.

In all other cases the various algorithms provided a significant improvement. In the low SNR cases the ICLEAN algorithm did not provide any improvement.

VI. Conclusions

In this paper we presented three techniques which significantly improve the CLEAN deconvolution algorithm

The use of the mass criterion as a tool for evaluating the performance of the CLEAN algorithm is justified for most practical cases as it is well correlated to the error in target location estimation. Using it imposes a PSF correlation method for the estimation of target parameters, which yields improved location estimates, both as a function of signal-to-noise and as a function of the average sidelobe level for most of the studied scenarios. It is still necessary to study the bounds on the residual target mass in various scenarios and the effects of incomplete knowledge of the system PSF on the overall performance of the CLEAN algorithm.

Sequence CLEAN has been found to perform better than coherent CLEAN, as expected. Coherent CLEAN is actually a subset of sequence CLEAN. Sequence CLEAN performs better at the cost of increased complexity and computation time.

The convergence as well as performance of sequence CLEAN depends on the value of m used as well as on the original image itself. For very high sidelobe levels it may be possible that the peak location error is such that cancellation of targets actually adds more target mass to the image. If real targets are completely lost in the sea of artifacts then it is impossible to recover the correct target locations.

The ICLEAN algorithm presented in (**12**) is a powerful tool in applying the CLEAN algorithm to an image where the main cause of errors in the estimation of target locations and amplitudes is the sidelobe interference. It is also very useful when main lobe interference is present. However, care should be taken when applying ICLEAN to images where noise is the main interfering source.

Acknowledgements

This work is supported by Grant No. N00014-93-0104 from the Office of Naval Research.

References

(1) A. J. Berkhout, "Least square inverse filtering and wavelet deconvolution", *Geophysics*, Vol. 42, pp. 1369–1383, 1977.

(2) B. Butkus, "Homomorphic filtering—theory and practice", *Geophys. Prosp.* Vol. 23, pp. 712–748, 1975.

(3) J. A. Hogbom, "Aperture synthesis with non-regular distribution of interferometer baselines", *Astron. Astrophys. Suppl.*, Vol. 15, pp. 417–426, 1974.

(4) J. Tsao and B. D. Steinberg, "Reduction of sidelobe and speckle artifacts in microwave imaging: the CLEAN technique", *IEEE Trans. Ant. and Prop.*, Vol. 36, No. 4, pp. 543–556, Apr. 1988.

(5) B. D. Steinberg, and H. Subbaram, "Microwave Imaging Techniques", Wiley, New York, 1991.

(6) S. R. De Graaf, "Parametric estimation of complex 2-D sinusoids", in "Proc. of the IEEE Fourth Annual Workshop on Spectrum Estimation and Modeling", pp. 391–396, Aug. 1988.

(7) D. L. Fried, "Analysis of the CLEAN Algorithm and implications for super-resolution", *J. Opt. Soc. Am. A*, Vol. 12, pp. 853–860, 1995.

(8) S. M. Kay, "Modern Spectral Estimation—Theory and Application", Prentice-Hall, Englewood Cliffs, NJ, 1988.

(9) R. Bose, B. D. Steinberg and A. Freedman, "A variation of the coherent CLEAN algorithm for contiguous targets", in "Adaptive Antenna Systems Symposium", IEEE Long Island Section, Nov. 1994.

(10) R. Bose, B. D. Steinberg and A. Freedman, "Sequence CLEAN: a deconvolution technique for reducing sidelobe artifacts in microwave images of continuous targets", in "Thirteenth Annual Benjamin Franklin Symposium on Antenna and Microwave Technology in the 1990s", May 1995.

(11) R. Bose, B. D. Steinberg and D. Carlson, "High resolution 2-D imaging with spectrally thinned wideband waveforms", in "2nd Int. Conf. on Ultra-Wideband, Short Pulse Electromagnetics", Weber Research Institute, Polytechnic University, New York, April, 1994.

(12) P. O. Husøy, "ICLEAN: a modified CLEAN algorithm used for feature extraction", in "NATO Workshop on Radar Imaging and Classification Techniques", FGAN Wachtberg-Werthoven, Germany, Jan. 1993.